



Sintigrafik Görüntülerden Tiroid Nodülleri için Bilgisayar Destekli Tanı Sistemi

Computer Aided Diagnosis System of Thyroid Nodules from Scintigraphic Images

Aysun Sezer ^{1*}, **Sadettin Emre Alptekin** ²

¹ Biruni Üniveristesi, Bilgisayar Mühendisliği, İstanbul, TÜRKİYE

²Galatasaray Üniveristesi, Endüstri Mühendisliği, İstanbul, TÜRKİYE

Sorumlu Yazar / Corresponding Author *: asezer@biruni.edu.tr

Geliş Tarihi / Received: 03.11.2022

Kabul Tarihi / Accepted: 12.01.2023

Atıf şekli/How to cite: SEZER, A., ALPTEKİN, S.E. (2023).Sintigrafik Görüntülerden Tiroid Nodülleri için Bilgisayar Destekli Tanı Sistemi .DEUFMD, 25(75), 559-567.

Araştırma Makalesi/Research Article

DOI:10.21205/deufmd.2023257504

Öz

Modern tıpta, anatomik bölgelerin segmentasyonu yoluyla görüntü tanıma ve tıbbi görüntüler kullanılarak hastalıkların otomatik olarak sınıflandırılması, çeşitli hastalıkların teşhisinde artan bir potansiyel role sahiptir. Tiroid sintigrafisi, tiroid bezi bozukluklarının teşhisi için kullanılan görüntüleme yöntemlerinden biridir. Çalışmamızda optimize edilmiş Bayesian yerel olmayan ortalama filtresi ile sintigrafik görüntülerinde benek gürültüsü azaltılmıştır. Tiroid bezi lokal bazlı aktif kontur yöntemi ile otomatik olarak segmentlere ayrıldı ve tiroid bezi patolojileri konvolüsyonel sinir ağları (CNN) ile sınıflandırıldı. Önerilen bilgisayar destekli tanı (CAD) sistemi, Histogramlar Piramidi Oryantasyon Gradyanları (PHOG), Gri Düzey Ortak Oluşum Matrisi (GLCM), Yerel Yapılandırma Modeli (LCP) ve Özellik Çantası (BoF) yöntemleriyle karşılaştırıldı. Tiroid bezinin sintigrafik görüntülerinin ortak patolojik paternleri, CNN tarafından %91.19 ile başarıyla sınıflandırıldı. Karşılaştırmalı yöntemler sırasıyla %7.61, %86.04, %88.91 ve %85.72 genel başarı oranları sağlayan PHOG, GLCM, LCP ve BoF yöntemleriydi. Önerilen CNN tabanlı otomatik teşhis sistemi, el yapımı yöntemlere kıyasla umut verici sonuçlar vermiştir.

Anahtar Kelimeler: Derin öğrenme, görüntü sınıflama, Aktif kontur, gürültü giderme, tiroid nodül, sintigrafik

Abstract

In modern medicine, image recognition via segmentation of anatomical regions and automatic classification of diseases using medical images has a growing potential role in diagnosis of various diseases. Scintigraphy of thyroid is one of the established imaging modalities for diagnosis of thyroid gland disorders. In our study, the speckle noise was reduced in the scintigraphy images with the optimized Bayesian nonlocal mean filter. The thyroid gland was automatically segmented by local based active contour method and the thyroid gland pathologies were classified with convolutional neural networks (CNN). The proposed computer aided diagnosis (CAD) system was compared with Pyramid of Histograms of Orientation Gradients (PHOG), Gray Level Co occurrence Matrix (GLCM), Local Configuration Pattern (LCP) and Bag of Feature (BoF) methods. The common pathological patterns of scintigraphic images of the thyroid gland were successfully classified by CNN with an overall success rate of 91.19%. The comparative methods were PHOG, GLCM, LCP and BoF methods which provided overall success rates of 7.61%, 86.04%, 88.91% and 85.72% respectively. The

proposed CNN based automatic diagnosis system provided promising results compared to handcrafted methods.

Keywords: *Deep learning, image classification, Active contour, noise reduction, thyroid nodules, Scintigraphic images*

1. Introduction

Thyroid nodules are among the most commonly encountered adult nodular lesions. 15-30% of these nodules have premalignant or transitional appearance and they have a 7% malignant transformation risk [1]. The incidence of thyroid cancer has been reported to increase 2.4-fold over the last 30 years. Thyroid carcinoma incidence increased 2.4 folds in the last three decades which is one of the leading compared to all other carcinomas [2].

Diagnosis of thyroid nodules depends on careful clinical examination and a series of imaging modalities. Thyroid ultrasonography (TUS) and thyroid scintigraphy are commonly used imaging modalities. Ultrasonography is useful in terms of defining the volume and localization of nodules. It is used as a guide to fine needle aspiration biopsy. Thyroid scintigraphy is a modality of nuclear medicine by which the functionality of thyroid tissue and nodules can be detected. Thyroid scintigraphy can sort the thyroid nodules according to their uptake as hypo or hyperactive. Besides its local diagnostic utilization scintigraphy is also useful in detecting distant metastasis of thyroid malignancy.

Common properties of ultrasound and scintigraphy images are speckle noise, textural intensity homogeneity and low contrast which render segmentation of thyroid nodules and computer aided detection (CAD) a challenging task. Literature yields various nodule detection studies from TUS images with Active Contour methods.

The topographic characteristics (shape, size, position) of a thyroid nodule is the key of diagnostic accuracy in computer aided diagnosis. Contour estimation accuracy is inversely related to the false positivity rate. KaundaI et. al. introduced an automated contour estimation method which incorporated spatial information for Level Set method for segmentation of ultrasound images. [3].

Another viable option for thyroid nodule detection from ultrasound images is Variable Background Active Contour (VBAC) model which offers multiple nodule detection without pre-

processing with more accuracy and less dependency to topographical variations but it is also highly dependent to the location of the initial contour [4,5].

The hybrid multi-scale model proposed by Tsantis et al. proposed another ultrasound segmentation model through fusion of the advantages of Hough transform and wavelet-based edge detection. This hybrid multi-scale model required shape information of the target nodule, with less performance on the asymmetrical forms like elliptic lesions and irregular contours of malignant transformations [6]. Iakovidis et al. proposed the fusion of Genetic Algorithm with VBAC(GAVBAC) which introduced automatic tuning of parameters to transcend the drawback of the VBAC [7]. Among the others Thyroid Boundary Detector was extracting and classifying features to provide the initial ROI [8]. On the other hand, Joint echogenicity texture model was able to evaluate the image intensity and distributions of linear binary model simultaneously by MumfordShah function with ability to discriminate hypo-hyper and iso-echoic nodules in TUS images. It was topographically more adaptable but not able to discriminate other anatomical structures like big vessels from the nodular tissue [4]. Another method called 'Thyroid nodule detector system' was able to detect nodules in TUS images and videos at high levels of accuracy [9]. The method of Ma et al. was based on active contour for edge detection and able to enhance contrast and establish smoothing, however, it was not automatized [10].

The model proposed by Ding et al. utilized thyroid elastograms and trained SVM with extracted statistical and textural features to diagnose malignant nodules with more than 95% accuracy although the defined threshold was hard [11]. Singh et al. Classified thyroid nodules by training SVM with extracted gray level co-occurrence matrix features. Their classification accuracy was not at the desired levels (84,62%) [12]. Acharya et al. used SVM to classify thyroid nodules with the fractal dimension, local binary pattern and laws texture energy pattern [13]. Encouraging results were obtained in these studies with handcrafted

feature extraction and with the help of a series of preprocessing operations. The challenge in those studies was extraction of features and to find the most effective of all. A CNN based method was proposed by Jinlian et al. in the manner of fusion of feature maps of two pre-trained CNN with different architectures to diagnose thyroid nodules. The CNN was trained with the Image Net database (15000 TUS images), then the learned feature maps were fused augmenting the accuracy up to 83,02% [14].

This manuscript proposes a CAD system for diagnosis of thyroid pathologies from scintigraphic images. The major problem in the image processing of thyroid scintigraphy images is the speckle noise. Therefore, noise reduction method had to be robust against speckle noise. Basic requirements to obtain a successful classification result in automatic segmentation is discrimination of vital tissues. OBFLM which is a speckle noise reduction method validated in ultrasound images, was used for speckle noise reduction in scintigraphy images [15].

As an important step of the proposed CAD system adequate size image patches from the desired localization were produced. An ideal image patch may be described as the part of image which contains vital structures excluding irrelevant parts of an image. In this study the Statistical level set (SLS) method was employed to segment necessary anatomical areas in the presence of inhomogeneous and noisy scintigraphy images [16]. The resulting images patches contain subgroups of diffuse homogeneous uptake, diffuse non-homogeneous uptake hyperactive nodule, hypoactive nodule and multinodular uptake. Defined regions of interest (ROI) were used to feed the proposed CNN. Discriminative features of the thyroid nodules were extracted in the defined ROI and utilized for classification of thyroid diseases.

There are increasing number of image classification [17, 18] and segmentation [19, 20] studies in the literature using CNNs. We conducted an extensive literature search on computer aided systems to help diagnosis of thyroid nodules, nevertheless we could not encounter any computer-based diagnosis system which automatically segment scintigraphic images and classify thyroid nodules based on CNN. The hypothesis of this study is that CNN is able to discriminate thyroid nodules as diffuse homogeneous uptake, diffuse

non-homogeneous uptake, hyperactive nodule, hypoactive nodule and multinodular uptake.

2. Material and Method

2.1. Thyroid abnormality and Data

Acquisition

Scintigraphic classification of thyroid nodules basically lies on their tendency to the given isotope. Hyperfunctionnal or hot nodules show increased uptake which resembles hot spots in images on the contrary hypofunctioning or cold nodules show less uptake compared to the surrounding tissue [21]. Thyroid scintigraphy gives valuable information about the thyroid gland in the presence of thyroid abnormality in the thyroid scan [22]. Fine needle aspiration biopsy (FNAB) with TUS guidance is used widely to rule out the malignancy. The scintigraphic characteristics of the nodules may be used as a means of assistance before FNAB because nodules with increased uptake (hot nodules) are generally benign and do not require FNAB, while less functioning nodules (cold nodules) may be malignant [23, 22]. Nowadays the primary function of the thyroid scintigraphy in the clinics is the work-up of a hyperfunctioning lesion. However, diagnosis of thyroid nodules of some patients with a normal TSH value can be delayed unless thyroid scintigraphy is done. Hegeds et al. stated that the risk of malignant thyroid nodules in the presence of normal TSH values to be higher than previously stated [22]

We have collected 954 scintigraphic images from Sisli Etfal Training and Research hospital. Our data set consist of 372 diffuse homogeneous uptake, 152 diffuse non-homogeneous uptake, 185 hyperactive nodule, 41 hypoactive nodule and 204 multinodular uptake.

Diffuse homogenous uptake group includes scintigraphic images of thyroid glands with even distribution of increased isotope uptake in the gland (Fig.1a). In a thyrotoxic patient this appearance is reported as Grave's disease. In this condition the gland is usually enlarged to some degree. Diffuse nonhomogenous uptake group includes images of enlarged thyroid glands with increased homogenous uptake in the glandular tissue but having distortions from the normal glandular shape, probably due to congenital or developmental conditions leading to anatomical distortions in the gland, periglandular pathologies or non-functioning regions of the glandular tissue itself (Fig.1b).

Hyperactive nodule group constitutes thyroid images with local increased uptake in the glandular tissue. The accumulation of isotope in the gland is mostly round in shape and usually does not cause so much distortion in the global structure of the gland (Fig.1c).

Thyroid gland images including a clearly visible solitary area of low accumulation of isotope in the glandular tissue were labeled as Hypoactive nodule. The general characteristics of images of lesions in these thyroid glands resemble Hyperactive nodule group although these lesions does not accumulate the given isotope (Fig.1d). Multi-nodular uptake group contains images of enlarged thyroid glands with heterogenous uptake due to multiple nodules which has differing degrees of isotope accumulation capacity (Fig.1e). Generally the outer borders of the gland is also distorted. Patients with toxic multi-nodular goiter were included in this group.

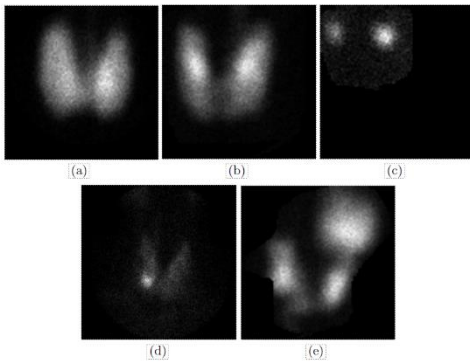


Figure 1. Demonstration of a) scintigraphic diffuse homogenous uptake, b) diffuse non-homogenous uptake, c) hyperactive nodule, d) hypoactive nodule and e) multi-nodular uptake images

2.2. Preprocessing of Scintigraphic Images Based on OBNLM

Noise reduction during medical image processing is a challenging problem due to tissue specific speckle noise and speckle artefacts which are hardly modelled. It is crucial to preserve the necessary structural information in the course of the noise reduction process. Non-Local Mean (NLM) Filter is a favorite image denoising method which creates several overlapping blocks out of the original image. It performs a similarity check in-between the reference block (Search window) and the remaining in terms of mean weight value which

renders noise reduction in the distant blocks as well as the blocks of the close proximity.

Originally created for Gaussian noise it can be operated on the speckle noise of the ultrasound images, either. Pierrick et al. Upgraded non-local mean filter and created optimized Bayesian non-local mean filter (OBNLM) by the help of Loupas noise model and Pearson distance measurement. Loupas noise model is one of the most successful speckle noise reduction models. Pearson distance measurement provided OBNLM in improving L2 similarity metric function in low signal to noise ratio images. OBNLM outperforms other well-known methods in the literature like anisotropic diffusion filter and local adaptive filter [24].

In this study we applied OBNLM method to scintigraphic images with the smoothing parameter ($h=3$) and search area size ($W=9$). Each center pixels x_{ik} of blocks B_{ik} were empirically estimated with the parameter $v_{b}(B_{ik})$ based on equations Eq. (1) and denoised scintigraphic images were obtained as demonstrated in Figure 2.

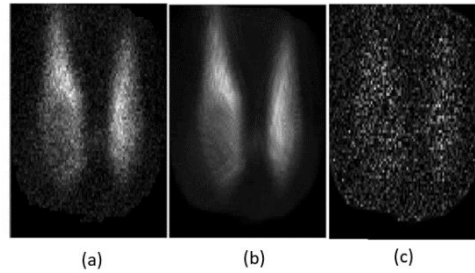


Figure 2. Demonstration of a) scintigraphic image of thyroid nodule, b) denoised scintigraphic image by OBNLM method with smoothing parameter ($h=3$) and search area size ($W=9$) and, c) corresponding residual image

$$v(B_{ik}) = \frac{\frac{1}{\Delta_{ik}} \sum_{j=1}^{|\Delta_{ik}|} v(B_j) p(u(B_{ik})|v(B_j))}{\frac{1}{\Delta_{ik}} \sum_{j=1}^{|\Delta_{ik}|} p(u(B_{ik})|v(B_j))} \quad (1)$$

2.3. Local Active Contour based Segmentation of Scintigraphic images

The inconvenience of piecewise constant function of Chan-Vese in segmentation of inhomogeneous images lead to the emergence of Statistical level set model (SLS). The working principle of SLS model is to label the target objects by means of multiple Gaussian

probability distributions of spatially varying means and variances. It is robust against inhomogeneous objects [16].

Probability density function $P(I(y)|\theta_i, B, x)$ utilises the different mean parameter $U_i(x)$ to define altering local region statistics in Eq. (2). Assuming the number of objects n in the image domain Ω , where Ω_i represents i^{th} object domain. The parameter x stands for the center of pixel of each local region Ox .

$$P(I(y)|\theta_i, B, x) = \frac{1}{\sqrt{2\pi\sigma_i}} \exp\left(-\frac{(I(y)-U_i(x))^2}{2\sigma_i^2}\right) \quad (2)$$

Statistically non-overlapping property of adjacent regions is required for a successful discrimination of all object regions in original image intensity domain $D(\tau)$. Mapping the image to another domain $R(\tau)$ by averaging image intensities within the predefined window size may be a solution for this problem. The following energy function was minimized with the regularized level set function ϕ .

$$E_{\theta, \beta, \phi}^J = \sum_{i=1}^N \int_{\Omega} F_i(y) M_i(\phi(y)) dy \quad (3)$$

SLS model attributes each pixel to more than one class resulting with identification of each object via Gaussian distribution of different means and variances. Transformed domain intensity is calculated by taking the average of the pixel intensities of the same class in the adjacent pixels. Classification results are less sensitive due to less overlapping statistics in the transformed domain compared to original one allows SLS method to be less sensitive to noise. In this manner, SLS method may be utilized as a bias correction tool due to its action of low pass filter [25]. The drawback of this method, however, is dependency on the initial contour. In this study all scintigraphic images were segmented with statistical level set method (Fig.3).

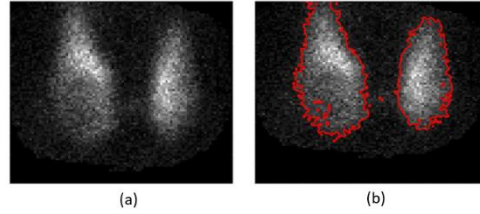


Figure 3. Demonstrate an original scintigraphic image and b) its segmentation result based on SLS method.

These feature maps are produced depending on the weights of the Neuronal inputs whose shared weights may serve as a filter for each map. The main function of them is to prevent over-fitting in other words to increase efficacy. The following layer is the activation layer after the convolutional layer. More complex features are extracted in the activation layer with the aid of nonlinear property of the activation layer. In the following pooling layer, inputs are statistically analyzed and the sensitivity of the image is decreased through shifting rectangles.

After determination of ROI different CNN architectures with different number of layers and size of the kernels in each layer were built. Each CNN configuration was evaluated by means of the influence of different size and quality datasets. By this way we determined the best CNN configuration to be employed in classification of thyroid nodules.

In the feature learning step the proposed architecture contained four convolutional and 3 max-pooling layers. In the first convolutional layer 101x101 image patches were given and 256 101x101 feature maps were generated. Next to the first convolutional layer we placed a rectified linear unit (ReLU) to replace negative feature map values with zero. In the second convolutional layer the kernel size was 7x7. It was employed to produce 192 feature maps of size 50x50. After convolution and activation Max-pooling operation was done in the feature maps taking the stride size 2 pixels. The third, fourth convolutional layers generated 64,128 and the last fully connected layer produced 128 feature maps of size 25x25, respectively.

We aimed to obtain the probability of each group from softmax function of the classification step of our proposed CNN as diffuse homogenous uptake, hyperactive nodule, hypoactive nodule and multinodular uptake.

2.3. Proposed convolutional neural network architecture

CNNs are multi-layered structures. There are 4 types of layers which process the gathered information from the neurons namely; convolutional, activation, pooling and fully connected. Every layer performs a different task in the network. Similar to the working principle of a mammalian retinal neuron, each neuron receives a local area of the image producing an overlapping representation of it in the convolutional layer. The function of the convolutional layer is to create feature maps. These feature maps are produced depending on the weights of the Neuronal inputs whose shared weights may serve as a filter for each map. The main function of them is to prevent over-fitting in other words to increase efficacy. The following layer is the activation layer after the convolutional layer.

More complex features are extracted in the activation layer with the aid of nonlinear property of the activation layer. In the following pooling layer, inputs are statistically analyzed and the sensitivity of the image is decreased through shifting rectangles. After determination of ROI different CNN architectures with different number of layers and size of the kernels in each layer were built. Each CNN configuration was evaluated by means of the influence of different size and quality datasets. By this way we determined the best CNN configuration to be employed in classification of thyroid nodules.

In the feature learning step the proposed architecture contained four convolutional and 3 max-pooling layers. In the first convolutional layer 101x101 image patches were given and 256 101x101 feature maps were generated. Next to the first convolutional layer we placed a rectified linear unit (ReLU) to replace negative feature map values with zero. In the second convolutional layer the kernel size was 7x7. It was employed to produce 192 feature maps of size 50x50. After convolution and activation Max-pooling operation was done in the feature maps taking the stride size 2 pixels. The third, fourth convolutional layers generated 64,128 and the last fully connected layer produced 128 feature maps of size 25x25, respectively. We aimed to obtain the probability of each group

from softmax function of the classification step of our proposed CNN as diffuse homogenous uptake, hyperactive nodule, hypoactive nodule and multinodular uptake.

3. Results

The focus of this study is to discriminate diffuse homogeneous uptake, diffuse non-homogeneous uptake, hyperactive nodule, hypoactive nodule and multinodular uptake classes from each other. The success of the proposed diagnosis system depends on its composition and architecture and selection of methods of feature extraction and thus the segmentation depends on a state of art. In this study we eliminated speckle noise based on OBNLM method in order to increase segmentation success. All scintigraphic images were successfully segmented with local active contour-based method after elimination of speckle noise by OBNLM method. Determined ROIs which contain all necessary anatomical regions were used to feature extraction and classification based on our proposed CNN.

The experiments of this study were held on a server which possessed NVIDIA Geforce GTX Titan X (6 GB on board memory) card. The algorithms of CNN worked in TensorFlow in Keras environment. Stability and reliability of the proposed system was checked by using 10-fold cross-validation method. The training set was 70% and the test set composed of the 30% of the whole data. Under these circumstances the accuracy rate of the computer aided diagnosis system was 91.19%. The success rates were 96.07% for homogeneous uptake, 94.0 % for

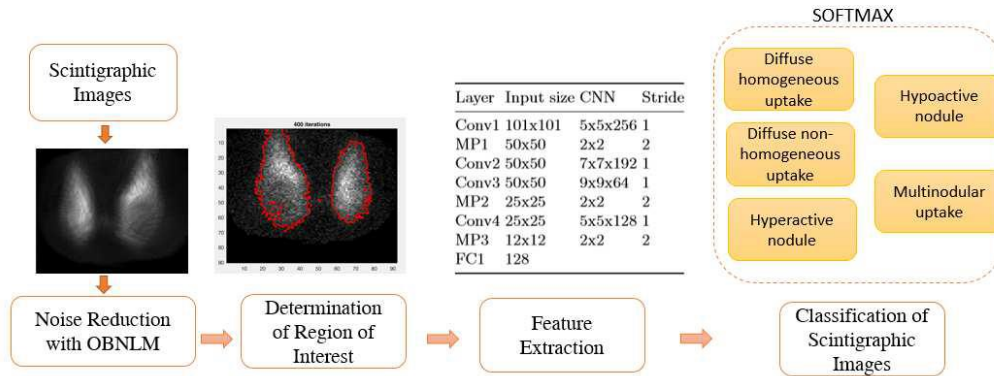


Figure 4. Flow of our proposed CAD system and Details of proposed CNN components (Conv: Convolutional Layer,MP: Max pooling layer, FC: Fully connected layer)

multinodular uptake and 92.97% for diffuse non homogeneous uptake which were at the desired level. However, proposed system was less performant with hyperactive and hypoactive nodules. The general characteristics of hyperactive nodule in these thyroid glands resemble hypoactive nodule although these lesions do not accumulate the given isotope (Fig.1d).

Lütfen görsel ile önceki ve sonraki paragraftan önce ve sonra boşluk eklenmemiş olduğunu “Satır ve Paragraf Aralığı” düzenleyicisi ile “Satır Aralığı Seçenekleri” bölümünden “Aralık” kısmında “Önce” ve “Sonra” değerlerinin 5nk olduğunu görerek kontrol ediniz.

Görsel içerisindeki veriler okunaklı olmalıdır. Eğer çalışmanızı İngilizce olarak sunmak istiyorsanız lütfen isimlendirmeleri grafik için graph, şekil için figure ve resim için picture olarak değiştirdiğinizden emin olunuz.

Table 1. Confusion Matrix of Proposed Convolutional Neural Network

Confusion Matrix of Proposed CNN for Thyroid Nodules					
	Homogeneous uptake	Diffuse non-homogeneous uptake	Hyperactive nodule	Hypoactive nodule	Multinodular uptake
Homogeneous uptake	96.07	1.62	2.43	0.65	0.80
Diffuse non homogeneous uptake	5.39	92.97	2.43	0.65	0
Hyperactive nodule	1.4	0	73.17	4.60	0.26
Hypoactive nodul	6.37	1.62	4.87	80.26	3.22
Multinodular uptake	3.43	0.54	4.87	7.89	94.08

For sake of comparison the dataset was classified with the state-of-the-art methods like PHOG, GLCM, local configuration and BoF (26-29). The local image and its spatial layout were

captured by PHOG by taking the parameters 3 levels of pyramid, 8 orientation bins between the range of (0-360). PHOG yielded 680 shape features.

We have extracted first and second order features for the symmetric GLCM created for offset=8 and orientation (θ : 0°, 45°, 90°, 135° Offset= 8). BoF was operated to generate 500 codebooks to delineate similar image patches. An unsupervised learning method was used to produce code words. The relative frequency of code words in each pixel was used to find thyroid nodules.

The overall success rates of these methods were 87.61%, 86.04%, 88.91% and 85.72% respectively (Table 2). The main constraint of present study is the restricted size of the dataset which theoretically has a negative impact on the efficiency of training thus the success rate.

Table 2. Overall accuracy rates of different methods for the classification of thyroid nodules

Methods of evaluation	Overall accuracy rate of classification (%)
PHOG evaluated on original data set	87.61
Bag of Feature evaluated on original data set	85.72
Gray level co-occurrence matrix	86.04
Local Configuration Pattern	88.91
Proposed CNN with original data set	91.19

The main constraint of present study is the restricted size of the dataset which theoretically has a negative impact on the efficiency of training thus the success rate.

6. Discussion and Conclusion

Thyroid hormones are one of the cardinal hormones of the human body regulate human metabolism. The follicular cells produce and store thyroid hormone. Presence of Iodine and tyrosine is essential for the thyroid gland function. Thyroid hormones can affect nearly all of the human cells. Therefore, pathologies in the gland lead to insufficiency or over production of thyroid hormones and result in conditions which affect the whole body.

This study showed that proposed CNN architecture classified thyroid nodules from scintigraphic images in 3 subclasses, successfully and especially in diffuse increased uptake subclass (96.7%). However, irregularities in the images of multinodular and non-homogenous uptake groups cause a relative decrease in the classification success as 94.08% and 92.97%, respectively. The results in hyperactive (73.17%) and hypoactive nodule (80.25%) groups were non-satisfactory. However, the overall success is still high in spite of irregular images and high noise in the images.

Comparison of the proposed CNN with the handcrafted methods also showed a satisfactory improvement with CNN classification.

Ultrasound studies which proposed handcrafted feature extraction and preprocessing methods like Singh et al. Achary et al, Ding et al. classified thyroid nodules with a range of reported success rates between 84.62%-95.2%. Jinlian et al. proposed a CNN on thyroid USG images with an overall success rate of 83.02%.

In this study classification of the thyroid nodules were achieved with the custom-made CNN architecture which produced very similar result with an experienced specialist. To our knowledge, it is the first study to classify scintigraphic images based on deep neural network, local configuration pattern and automatically classification of subclass of thyroid nodules as diffuse homogeneous uptake, diffuse non-homogeneous uptake, hyperactive nodule, hypoactive nodule and multi-nodular uptake classes.

The proposed automatic classification system is performant on thyroid scintigraphy images. Authors proposed a computer aided diagnosis system without human intervention to diagnose thyroid pathologies. Performance of the of the proposed system surpassed the traditional

methods and provided comparable results with an experienced evaluator. Nuclear medicine practitioners, endocrinologist and surgeons may benefit from this computer aided diagnosis system in decision making. The current study reports positive impact of noise reduction in the classification of scintigraphic images using the OBFLM method. Clinical use of such systems might facilitate daily practice and improve the quality of life for both the practitioners and the patients.

7. Ethics committee approval and conflict of interest statement

Ethics committee approval is not required for this article.

"There is no conflict of interest with any person/institution in this study"

References

- [1] Vorländer, C., Wolff, J., Saalabian, S., Lienenlücke, R. H., Wahl, R. A. 2010. Real-time ultrasound elastography -a noninvasive diagnostic procedure for evaluating dominant thyroid nodules. *Langenbeck's archives of surgery, Cilt. 395(7)*, s. 865-871. DOI: 10.1007/s00423-010-0685-3
- [2] Zhu, C., Zheng, T., Kilfoy, B. A., Han, X., Ma, S., Ba, Y., Bai, Y., Wang, R., Zhu, Y., Zhang, Y. 2009. A birth cohort analysis of the incidence of papillary thyroid cancer in the United States, 1973–2004. *Thyroid, Cilt.19(10)*, s. 1061-1066. DOI: 10.1089/thy.2008.0342
- [3] Koundal, D., Gupta, S., Singh, S. 2016. Automated delineation of thyroid nodules in ultrasound images using spatial neutrosophic clustering and level set. *Applied Soft Computing, Cilt. 40*, s. 86-97. DOI: 10.1016/j.asoc.2015.11.035
- [4] Savelonas, M. A., Iakovidis, D. K., Legakis, I., Maroulis, D. 2008. Active contours guided by echogenicity and texture for delineation of thyroid nodules in ultrasound images. *IEEE Transactions on Information Technology in Biomedicine, Cilt. 13(4)*, s. 519-527. DOI: 10.1109/TITB.2008.2007192
- [5] Maroulis, D. E., Savelonas, M. A., Iakovidis, D. K., Karkanis, S. A., Dimitropoulos, N. 2007. Variable background active contour model for computer-aided delineation of nodules in thyroid ultrasound images. *IEEE Transactions on Information Technology in Biomedicine, Cilt. 11(5)*, s. 537-543. DOI: 10.1109/TITB.2006.890018
- [6] Tsantis, S., Dimitropoulos, N., Cavouras, D., Nikiforidis, G. 2006. A hybrid multi-scale model for thyroid nodule boundary detection on ultrasound images. *Computer methods and programs in biomedicine, Cilt. 84(2-3)*, s. 86-98. DOI: 10.1016/j.cmpb.2006.09.006
- [7] Iakovidis, D. K., Savelonas, M. A., Karkanis, S. A., Maroulis, D. E. 2007. A genetically optimized level set approach to segmentation of thyroid ultrasound images. *Applied Intelligence, Cilt. 27(3)*, s.193-203. DOI: 10.1007/s10489-007-0066-y

- [8] Keramidas, E. G., Iakovidis, D. K., Maroulis, D., Karkanis, S. 2007. Efficient and effective ultrasound image analysis scheme for thyroid nodule detection. In International Conference Image Analysis and Recognition, August 22-24, Montreal, 1052-1060
- [9] Keramidas, E. G., Maroulis, D., Iakovidis, D. K. 2012. TND: a thyroid nodule detection system for analysis of ultrasound images and videos. *Journal of medical systems*, Cilt. 36(3), s. 1271-1281. DOI: 10.1007/s10916-010-9588-7
- [10] Ma, J., Luo, S., Dighe, M., Lim, D. J., Kim, Y. 2010. Differential diagnosis of thyroid nodules with ultrasound elastography based on support vector machines. *IEEE International Ultrasonics Symposium 11-14 October*, 1372-1375.
- [11] Ding, J., Cheng, H., Ning, C., Huang, J., Zhang, Y. 2011. Quantitative measurement for thyroid cancer characterization based on elastography. *Journal of Ultrasound in Medicine*, Cilt. 30(9), s. 1259-1266. DOI: 10.7863/jum.2011.30.9.1259
- [12] Singh, N., Jindal, A. 2012. Ultra sonogram images for thyroid segmentation and texture classification in diagnosis of malignant (cancerous) or benign (non-cancerous) nodules. *Int. J. Eng. Innov. Technol.*, Cilt. 1, s. 202-206.
- [13] Acharya, U. R., Sree, S. V., Krishnan, M. M. R., Molinari, F., Garberoglio, R., Suri, J. S. 2012. Non-invasive automated 3D thyroid lesion classification in ultrasound: a class of ThyroScan™ systems. *Ultrasonics*, Cilt. 52(4), s. 508-520. DOI: 10.1016/j.ultras.2011.11.003
- [14] Ma, J., Wu, F., Zhu, J., Xu, D., Kong, D. 2017. A pre-trained convolutional neural network based method for thyroid nodule diagnosis. *Ultrasonics*, Cilt. 73, s. 221-230. DOI: 10.1016/j.ultras.2016.09.011
- [15] Coupé, P., Hellier, P., Kervrann, C., Barillot, C. 2009. Nonlocal means-based speckle filtering for ultrasound images. *IEEE transactions on image processing*, Cilt. 18(10), s. 2221-2229. DOI: 10.1109/TIP.2009.2024064
- [16] Zhang, K., Zhang, L., Lam, K. M., Zhang, D. 2015. A level set approach to image segmentation with intensity inhomogeneity. *IEEE transactions on cybernetics*, Cilt. 46(2), s. 546-557. DOI: 10.1109/TCYB.2015.2409119
- [17] Ma, J., Wu, F., Jiang, T. A., Zhu, J., Kong, D. 2017. Cascade convolutional neural networks for automatic detection of thyroid nodules in ultrasound images. *Medical physics*, Cilt. 44(5), s.1678-1691. DOI: 10.1002/mp.12134
- [18] Arevalo, J., González, F. A., Ramos-Pollán, R., Oliveira, J. L., Lopez, M. A. G. 2016. Representation learning for mammography mass lesion classification with convolutional neural networks. *Computer methods and programs in biomedicine*, Cilt. 127, s. 248-257. DOI: 10.1016/j.cmpb.2015.12.014
- [19] Yu, L., Guo, Y., Wang, Y., Yu, J., Chen, P. 2016. Segmentation of fetal left ventricle in echocardiographic sequences based on dynamic convolutional neural networks. *IEEE Transactions on Biomedical Engineering*, Cilt. 64(8), s. 1886-1895. DOI: 10.1109/TBME.2016.2628401
- [20] Chen, H., Ni, D., Qin, J., Li, S., Yang, X., Wang, T., Heng, P. A. 2015. Standard plane localization in fetal ultrasound via domain transferred deep neural networks. *IEEE journal of biomedical and health informatics*, Cilt. 19(5), s. 1627-1636. DOI: 10.1109/JBHI.2015.2425041
- [21] Corvilain, B., Van Sande, J., Dumont, J. E., Bourdoux, P., Ermans, A. M. 1998. Autonomy in endemic goiter. *Thyroid*, Cilt. 8(1), s. 107-113. DOI: 10.1089/thy.1998.8.107
- [22] Hegedüs, L. 2004. The thyroid nodule. *New England Journal of Medicine*, Cilt. 351(17), s.1764-1771. DOI: 10.1056/NEJMc031436
- [23] Sarkar, S. D. 2006. Benign thyroid disease: what is the role of nuclear medicine?. In *Seminars in nuclear medicine*. Cilt. 36-3, s 185-193). DOI: 10.1053/j.semnuclmed.2006.03.006
- [24] Zhang, J., Wang, C., Cheng, Y. 2015. Comparison of despeckle filters for breast ultrasound images. *Circuits, Systems, and Signal Processing*, Cilt. 34(1), s.185-208. DOI: 10.1007/s00034-014-9829-y
- [25] Zhang, K., Zhang, L., Zhang, S. 2010. A variational multiphase level set approach to simultaneous segmentation and bias correction. *IEEE International Conference on Image Processing, Hong Kong, 26-29 September*, 4105-4108
- [26] Bosch, A., Zisserman, A., Munoz, X. 2007. Representing shape with a spatial pyramid kernel. In *Proceedings of the 6th ACM international conference on Image and video retrieval, Amsterdam, July 5-7*, 401-408.
- [27] Soh, L. K., Tsatsoulis, C. 1999. Texture analysis of SAR sea ice imagery using gray level co-occurrence matrices. *IEEE Transactions on geoscience and remote sensing*, Cilt. 37(2), s. 780-795. DOI: 10.1109/36.752194
- [28] Guo, Y., Zhao, G., Pietikäinen, M. 2011. Texture classification using a linear configuration model based descriptor. *BMVC*. s. 1-10. DOI: 10.5244/C.25.119
- [29] Deselaers, T., Pimenidis, L., Ney, H. 2008. Bag-of-visual-words models for adult image classification and filtering. In *2008 19th International Conference on Pattern Recognition*. Tampa, 08-11 December, 1-4